THE ENERGETIC ION COMPOSITION SPECTROMETER (EICS) FOR THE DYNAMICS EXPLORER-A

E. G. SHELLEY, D. A. SIMPSON, T. C. SANDERS, and E. HERTZBERG
Lockheed Palo Alto Research Laboratories, 94304 Palo Alto, California, U.S.A.

and

H. BALSIGER and A. GHIELMETTI
Physikalisches Institut, University of Bern, 3017 Bern, Switzerland

(Received 20 April, 1981)

Abstract. The energetic ion composition spectrometer (EICS) on the DE-A spacecraft is a high sensitivity (≈ 1 cm^2-sr-eV), high resolution ($M/\Delta M \gtrsim 10$ FWHM at focus) instrument. It covers the entire mass range from less than 1 amu/e to greater than 150 amu/e in 64 mass channels at each of 32 energy per charge steps covering the range from 0 to approximately 17 keV/e. The measurements obtained from this instrument will be used primarily to investigate the coupling between the magnetosphere and the ionosphere via the auroral acceleration region. Additional uses of the data will be to investigate the ring current loss processes, the coupling of the dayside cusp particles to the magnetosheath, and the tracing of artificially injected ions.

1. Introduction

The measurement of the hot plasma composition within the auroral acceleration regions is an essential element in furthering our understanding of the mass and energy coupling between the magnetosphere and the ionosphere. The Dynamics Explorer-A (DE-A) spacecraft is the first to carry suitable instrumentation into a critical region of altitude (>8000 km) at high magnetic latitudes. Ion composition measurements from the polar orbiting S3-3 satellite with apogee at 8000 km revealed the existence of large fluxes of energetic ($\approx$keV) ionospheric O^+ and H^+ ions flowing upward into the magnetosphere on auroral field lines [1, 2]. Energetic ion composition measurements on the GEOS-1 and GEOS-2 satellites lead to the conclusion that a significant fraction of the hot equatorially trapped magnetospheric plasma is also of ionospheric origin [3]. Similar measurements from the ISEE-1 spacecraft have shown that field aligned streams of hot ionospheric ions permeate the plasmasheet as well as the tail lobes out to 23 earth radii [4, 5]. Recent observations of field aligned bursts of energetic ionospheric O^+ and H^+ ions near the equator by the SCATHA energetic ion mass spectrometer clearly indicated that significant perpendicular heating of the ion beams takes place above the maximum altitude at which they were observed by the S3-3 satellite (≈ 8000 km) [6].

One of the primary objectives of the energetic ion composition spectrometer (EICS) on the DE-A spacecraft is to measure the energy and pitch angle distributions of the principal mass constituents (O^+, H^+) of the upward flowing ions from the auroral acceleration region. The increased sensitivity of the EICS relative to the S3-3 spectrometer combined with the higher spin rate and higher altitude range of the DE-A spacecraft will represent a significant advance in the measurement of the upflowing ion distri-

Space Science Instrumentation **5** (1981) 443–454. 0377–7936/81/0054–0443 $01.80.

butions. These measurements are essential to an understanding of both the energy and mass coupling between the magnetosphere and the ionosphere. The simultaneous measurement of these ion distributions together with measurements of the associated auroral forms, waves, hot electron distributions, ambient ionospheric plasma and the electric currents will significantly improve our understanding of the auroral processes as well as related phenomena such as auroral kilometric radiation (AKR).

Another important area of investigation will be the dayside cusp region. The combination of the DE-A orbit and its complement of instrumentation offers a unique opportunity to improve our understanding of the entry of magnetosheath plasma through the dayside cusp and its interaction with the magnetospheric and ionospheric plasmas. Measurements of the relative latitudinal and energy distributions of the H^+ and He^{2+} ions can be used to infer both the parallel and convection electric fields which have acted on the plasma during its transport from the solar wind [7, 8]. The EICS will also monitor the upflowing O^+ ions being accelerated in the low altitude cusp region [9].

Other objectives include studies of ion acceleration over the polar caps, mass depen-

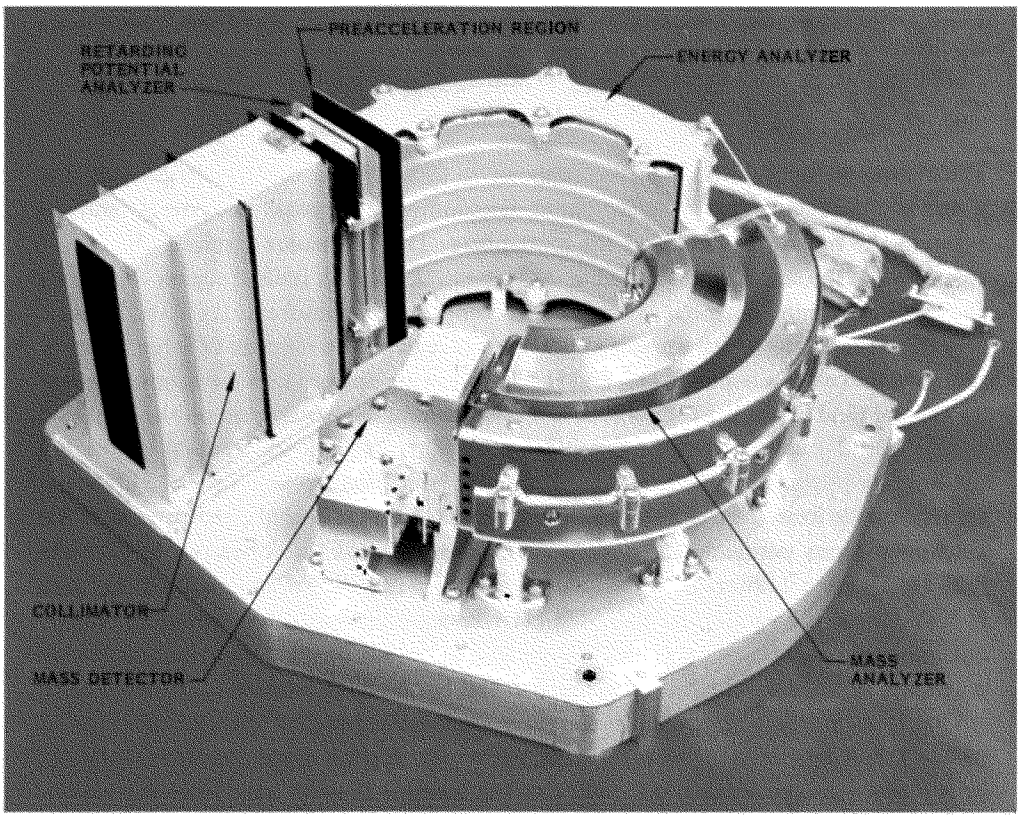

Fig. 1. A photograph of the ion optics section of the EICS with its hermetically sealed cover removed. Various components of the system are indicated. In the flight configuration only the front aperture of the collimator is exposed.

dence of the ring current loss processes, the plasmasphere filling process, and the support of tracer experiments utilizing artificially injected particles.

2. Instrument Description

2.1. Ion optics

The ion optics of the EICS are nearly identical to those of the ISEE spectrometers [10] which were based on the earlier design of the GEOS-1 and GEOS-2 spectrometers [11]. Figure 1 is a photograph of the ion optics section of the EICS with its hermetically sealed cover removed and Figure 2 is a schematic of the optical path, approximately to scale. The ions enter through the collimator which limits both the azimuthal and elevation angles of acceptance. The azimuthal limits are nearly constant at approximately $\pm 5.5°$ while the limit on the elevation angle for the mass analyzed beam varies from approximately $\pm 25°$ for cold (eV) plasma to $\pm 7.5°$ at 17 keV. This energy dependence results from the preacceleration of the ions within the spectrometer. The angular limits on the

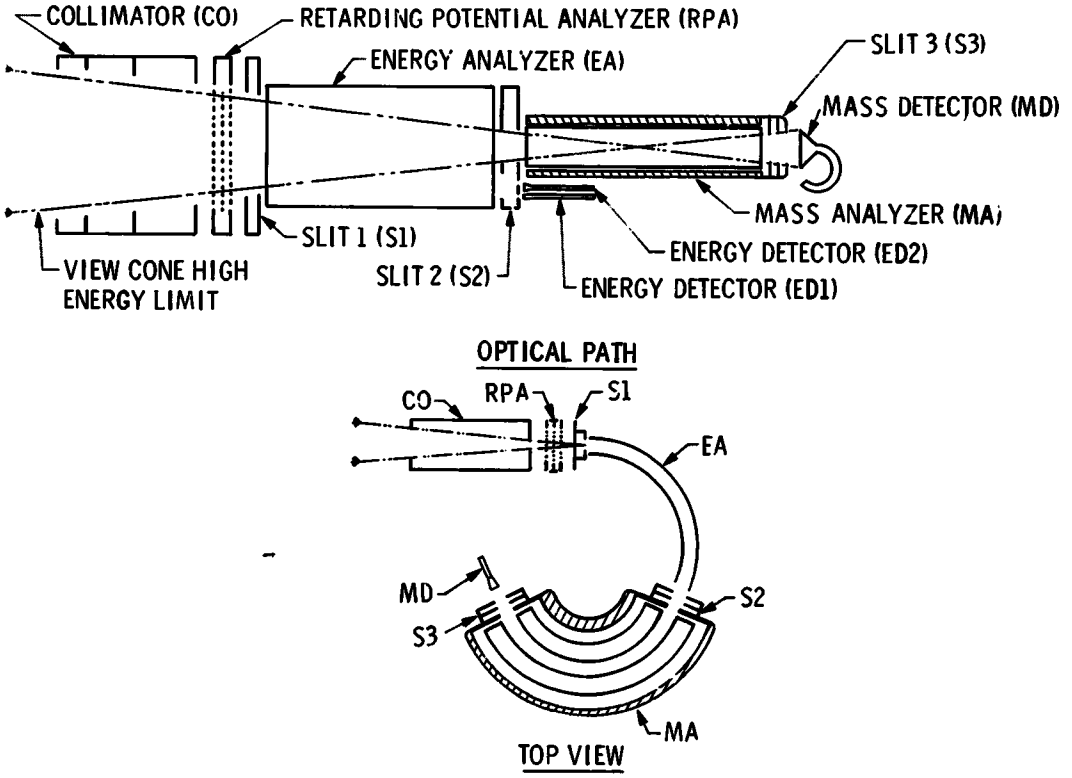

Fig. 2. A schematic diagram of the EICS ion optics, approximately to scale. The upper portion is a section taken along the central ray path of the ions. The limiting ion trajectories shown are for very energetic ions only. Due to the −2960 volt acceleration between the RPA and S1, all ions are refracted at this point. See the text for details.

ions reaching the energy detectors are comparable, but are offset due to the vertical displacement of these detectors. Immediately following the collimator, the ions pass through a three-grid retarding potential analyzer (RPA). The first and third grids are grounded while a positive potential (V_{RPA}) is applied to the central grid. This potential is programmable in 32 steps such that,

$$V_{RPA,k} \approx [0.5(1.185)^k - 0.5] \text{ Volts}, \qquad 0 \leq k \leq 31. \tag{1}$$

After passing through the RPA, all positive ions are accelerated through a potential of approximately -2960 V. The remainder of the analysis system is maintained at this centerline potential. After this preacceleration, the ions pass through the object slit (S1) and enter the cylindrical electrostatic energy analyzer (EA). The EA is programmable in 32 energy-per-charge steps covering the range from 3000 eV/e to 20 000 eV/e internal to the analyzer. In terms of ion energies outside the analyzer prior to the preacceleration the mean energy per charge ($\overline{U}_i$) of ions on the ith step is given by

$$\overline{U}_i = [3000(1.0631)^i - 2960] \text{ eV/e}, \qquad 1 \leq i \leq 31. \tag{2}$$

The FWHM energy passband is approximately 5% of the internal energy, so that

$$\Delta U_i(\text{FWHM}) \approx 150(1.0631)^i \text{ eV/e}, \qquad 1 \leq i \leq 31.$$

It will be noted that $\Delta U_i/\overline{U}_i$ increases significantly at low energies (i.e., small step numbers). The lowest step ($i = 0$) passes all ions with energies greater than zero (i.e., those cold ions which overcome any spacecraft potential and enter the collimator section with velocity equal to the satellite velocity) and less than approximately 115 eV/e. Thus in this step the RPA can be utilized to control the net energy per charge passband to

$$V_{RPA,k} \leq U_{0,k} \lesssim 115 \text{ eV/e}, \qquad 0 \leq k \leq 31$$

where again $V_{RPA,k}$ is the kth voltage step on the RPA.

As indicated in Figure 1, there are two channel electron multipliers (ED1 and ED2) positioned below the mass analyzer immediately following the EA. Each ED intercepts essentially the same component of the ion flux which enters the mass analyzer (MA) through slit S2. However, these detectors are sensitive to all ions within the energy passband, independent of mass. The sensitive area of ED1 is approximately 0.1 that of ED2. Only one of these detectors is operated at any given time; the choice is made according to the sensitivity desired and is programmable through the instrument control system which is discussed below. The sensing areas of the channel electron multipliers are biased to approximately -3 kV to minimize the variation in detection efficiency with variation in mass and energy.

The central portion of the ion flux passing through the EA enters the MA through slit S2. The MA consists of a second cylindrical electrostatic deflection system suspended inside a magnetic field of approximately 960 G with the E-field and B-field very nearly perpendicular everywhere. The fields are so arranged that their forces on the ions are additive. The equation of motion for a normally incident ion traveling on the central line of the MA is

$$\frac{2U}{R} = E_r(R) + \left(\frac{2Ze}{Mm} U\right)^{1/2} B_z, \tag{3}$$

where (in MKS units) E_r is the radial electric field at R, Z is the ion charge state, M is the atomic weight (in amu), e is the elementary charge, m is the atomic mass unit, and B_z is the perpendicular magnetic field intensity. The internal ion energy per charge U is fixed by the EA. At each energy step, the electric field in the MA is programmable in 64 linear steps in such a way that the same mass always appears at the same step number according to the equation,

$$(M/Q)_j = 0.761\left(1 - \frac{j}{63}\right)^{-2}, (0 \leq j \geq 63), \tag{4}$$

where $(M/Q)_j$ is the mean mass per unit charge (in amu/e) passed through the image slit (S3) on the jth mass step. The ions exiting through the image slit S3 are detected by a high current channel electron multiplier (MD). As was the case with ED1 and ED2, the sensitive area (front end) of the MD is biased at approximately -3 kV to improve the detection efficiency.

The optical design of the system is such that the EA alone is in angular focus and is energy dispersive at S2. Due to the fixed magnetic field in the MA, its focal properties are energy and mass dependent. Along the focus line, which runs from high energy-low mass to low energy-high mass, the combined EA-MA system is both energy and angle focusing at S3. Above the focus line the mass resolution slowly degrades (See Figure 5) but below the focus line the resolution remains nearly constant or improves slightly. The latter results primarily from the preacceleration which significantly decreases the angular divergence of the collimated ion beam inside the analyzer. The mass resolution will be discussed in more detail in the section on calibrations.

2.2. Instrument, control

As discussed above, the ion optics consist of a series RPA, EA, and MA. There is a voltage step control register associated with each of these series elements. The RPA and EA voltage settlings are dependent only upon their own 5-bit codes according to Equations (1) and (2) respectively, while the MA voltage is dependent on both the EA 5-bit code and its own 6-bit code as is suggested by Equation (3) where the field $E(r)$ is a function of both the energy-per-charge (U) and the mass (M). The instrument operates on a hierarchy of three basic time scales. The lowest (T1) is one-half minor frame ($\approx 1/32$ s). During this time period all analyzer control parameters are frozen and count rates are accumulated from either ED1 or ED2, whichever is selected, and from two discriminator levels from the MD. These three count rates are log compressed to 8 bits each and transmitted, together with an 8-bit STATUS word, during the succeeding T1 interval. The instrument could in theory switch from any one set of RPA, EA, and MA codes to any other set from one T1 to the next. It is limited only by the ability to program the respective registers and the need to know these settings in order to interpret data. For practical reasons, all but one of the three analyzer codes is held constant for a minimum

period T2 which is equal to 16 T1 intervals (0.5 s). The selection of which of the three codes is permitted to vary on a T1 time scale is dependent on the mode of operation. Independent of which code is selected, the code for the varied parameter makes up 6 bits of the 8-bit STATUS word. All other instrument configuration parameters, except for those alterable only by direct command, are transmitted on a T2 time scale. The remainder are transmitted on a T3 time scale which is equal to 8 T2 intervals (4 s). The T2 and T3 interval parameters are transmitted via the two remaining bits of the STATUS word. The combined instrument STATUS information is sufficient to completely reconstruct the instrument configuration for any given measurement.

Due to the large parameter space of the combined RPA, EA and MA (4096 combinations since the RPA is operable only in the lowest EA step), it would require 128 s to scan the entire matrix. This type of measurement cycle is clearly impractical for auroral zone phenomena which are expected to have temporal scales (in the spacecraft frame) of this order or less. Also, the distributions of interest will typically have strong pitch angle dependencies. Fortunately, many of the objectives of the EICS can be met by taking measurements over small subsets of the total 4096 elements in the energy-mass matrix. The instrument control system is designed to offer maximum feasible flexibility in the selection of these subsets consistent with reasonable limits on complexity. A block diagram of the system is shown in Figure 3. The primary instrument mode control is via the 1024 word (6-bit) random access memory (RAM) which is reprogrammable via minor mode command. The RAM is organized into 51, 20-word blocks of memory, each of which consists of a one word mode identifier, two control words, one fixed parameter and 16 variable parameters. The mode identifier is a passive 6-bit code which is included in the telemetry stream as an aid in data analysis. The control words affect the implementation of the fixed and variable parameters as well as other instrument functions such as the selection of detector deadtime, threshold and sensitivity. Other than those instrument parameters which are controlled by registers external to the RAM, such as detector bias voltages, a single block of memory makes up a stand-alone set of measurement instructions. The resulting sequence of measurements can vary considerably from memory block to memory block and the period of time required to execute the instruction sets varies from a minimum of one-half second to a maximum of 128 s. Any number of memory blocks may be strung together to make up a desired science mode by setting a flag in each memory block to indicate whether to proceed to the next memory block or to recycle to the first block in the sequence.

The energy-mass sequence of each memory block falls into one of two classes, DRUM or RAM, according to the source of the mass code. Each of these classes is further broken down into two energy modes, EA and RPA, according to whether the energy code controls the cylindrical electrostatic analyzer (EA) or the retarding potential analyzer (RPA). In a DRUM sequence, the mass analyzer continuously sequences through the four MSTEP DRUM words (see Figure 3), recycling 8 times per s. The EA or RPA, depending on the energy mode, sequences through the 16 variable parameters of the memory block, advancing one element every 6 s ($\approx$ 1 spin period). A DRUM sequence always takes 96 s to complete. It should be noted that the four MSTEP DRUM words

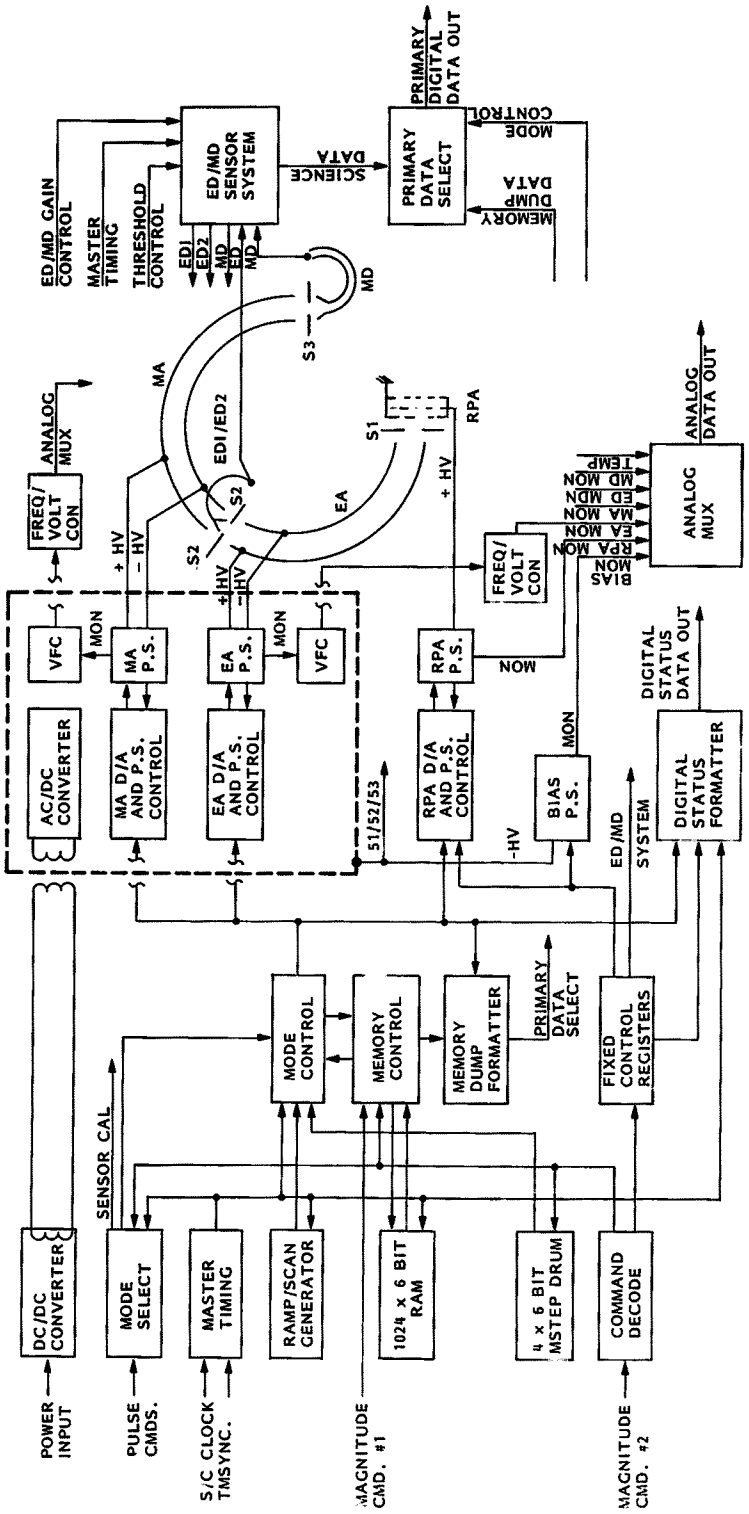

Fig. 3. Block diagram of the EICS. See text.

can only be altered by direct command (i.e., they are not altered by the RAM). Thus if more than one memory block involves a DRUM sequence the same mass steps will be covered, but the energy sequence can be altered. An example of a DRUM sequence for auroral plasma studies would involve programming the four MSTEP DRUM words to mass steps corresponding to H^+, $^4He^+$, $^4H^{2+}$, and $^{16}O^+$ respectively and programming the 16 variable parameters to 15 electrostatic analyzer steps spanning the full energy range from near 0 to 17 keV plus one background step (analyzer voltage off). With this programming a complete pitch angle distribution (7.5° resolution) is measured for each of the four mass components at one energy during a single spin period and in 16 spin periods (96 s) a complete energy-pitch angle distribution is measured for each of the four masses.

In a RAM sequence, either the mass code or the energy code is held constant at the value of the fixed parameter for the duration of the sequence while the alternate code, energy or mass, sequentially takes on the values of the 16 variable parameters. Each of the variable parameters is held for a period ranging from one T1 ($\approx 1/32$ s) to 256 T1 intervals (8 s) in accordance with the dwell parameter of the associated control words. An example of the utilization of RAM sequences is the science mode designed to acquire energy-pitch angle distributions for two mass constituents (H^+ and $^{16}O^+$) at the maximum time resolution. This is accomplished by programming 24 memory blocks with the fixed parameter set at the mass step for H^+ and 24 memory blocks with the fixed parameter set at the mass step for $^{16}O^+$. In 12 consecutive memory blocks associated with each of the two masses, the 16 variable parameters are programmed to repeat a set of 8 energy steps twice. Each variable parameter is held for the minimum time period (1/32 s) so that an eight point energy spectrum is repeated four times per second or approximately every 15° of satellite rotation. By programming the other 12 memory blocks with 8 additional energy steps, interleaved with the first set of 8, it is possible to acquire a 16 by 24 energy-angle distribution for both H^+ and $^{16}O^+$ in 24 s.

More complex science modes can be created by stringing together DRUM sequences and RAM sequences. Any number of separate science modes can be stored in the RAM at a given time, limited only by the total number of memory blocks available (51). The desired mode is selected by specifying (via command) the starting address of its first memory block. A complete reprogramming of the RAM requires 256 minor mode commands.

In addition to the modes which utilize the RAM there are two firm modes, LOADSCAN and LOAD DRUM. The former is the default mode at instrument turn-on but either is selectable by pulse command. The instrument must be in one of these modes to enable the reprogramming of the RAM. In the LOADSCAN mode the EA is scanned up on even steps then down on odd steps at the maximum rate while the mass steps ramp over the full 64 step range, incrementing one per EA scan (1 s). The full cycle repeats every 64 s. The LOAD DRUM mode is similar to the DRUM sequence described above, except that the EA follows the pattern of scanning up on even steps and down on odd steps, as in the LOADSCAN mode, but advancing only one step per spin period.

There are also two 'engineering modes' which can be initiated by pulse commands.

One is a RAM DUMP mode in which the contents of the RAM are transmitted in place of the science data. A total image of the RAM is transmitted each major frame (8 s). The second engineering mode is an automatic instrument calibration cycle. In this mode the gains of the channel electron multipliers are measured by cycling through discriminator thresholds and the pulse counting system is checked by feeding charge pulses to the inputs of the preamplifiers. At the completion of either of these modes (64 s) the system automatically returns to the previously selected science mode.

3. Calibration

Due to the fixed magnetic field, the focal properties of the EICS are both energy and mass dependent. The design was based on detailed ray tracing procedures; however, in a complex system of this type it is essential to perform relatively detailed laboratory calibrations to establish the actual response characteristics of the instrument. In addition, it is frequently desirable to measure the distribution of a minor constituent whose concentration relative to the major constituents is only a fraction of a percent. Thus it is essential to determine any possible internal scattering or 'ghosting' to the order of 10^{-4} or better.

All calibrations of the EICS were performed at the calibration facility at the University of Bern. This facility was specifically designed to calibrate energetic ion mass spectrometers. It can produce either mixed mass or mono-mass beams which are either mono-energetic or have a controllable energy spread sufficient to uniformly fill the instrument energy passband. The system provides various beam diagnostics including a beam profile monitor, an absolute current monitor and a continuous feedback monitor to maintain a constant beam intensity. The instrument mount is programmable in two angular dimensions so that the direction of incidence relative to the instrument aperture is completely controllable.

The calibration was performed in two steps. First the energy response characteristics were measured by stepping monoenergetic beams over representative energy steps covering the full energy range of the EICS. Following this, the detailed mass-angle response characteristics were measured with broad energy, mono-mass beams which uniformly filled the previously measured energy passbands. This involved measuring the response over the full 64 step mass range at each element of an angular matrix covering the full angular range of the instrument. This typically involved recording 5000 to 10 000 count rates from each of three accumulators, (i.e. ED rates plus two MD rates). This set of measurements was performed at each of 9 energy steps for 5 different mass components ($^1H^+$, $^1H_2{}^+$, $^4He^+$, $^{20}Ne^+$, and $^{131}Xe^+$). In addition, limited measurements were made for $^{20}Ne^{3+}$ and $^{131}Xe^{2+}$. To accomplish these measurements in a reasonable period of time, the instrument mount platform control was interfaced with the EICS experiment control system and all data were recorded on floppy discs. Figure 4 shows a representative set of mass response curves resulting from integrating the responses over the two dimensional field of view. These particular data were taken at energy step 8 ($\approx$ 1.94 keV mean energy). Figure 5 shows the measured full width at half

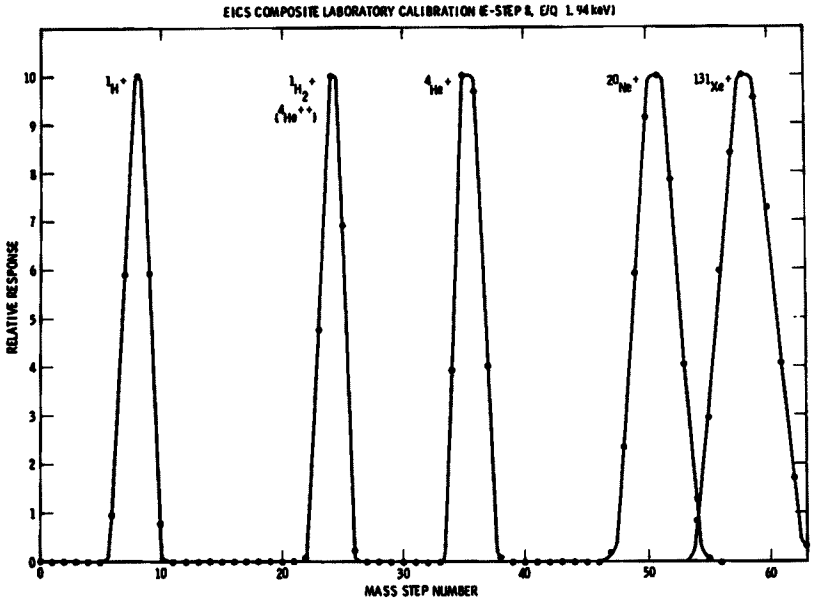

Fig. 4. Representative mass resolution line shapes for the EICS. Each mass line was determined independently during the instrument calibration by integrating the instrument response over velocity space.

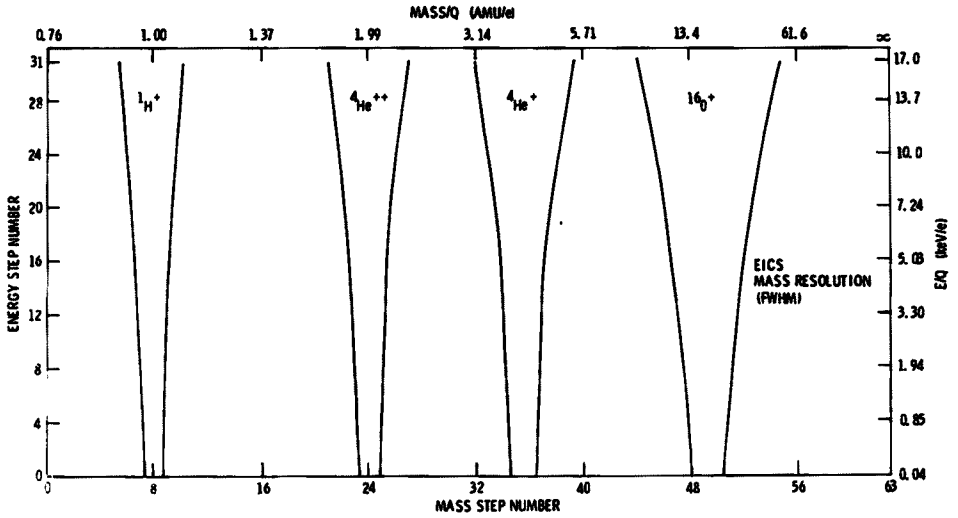

Fig. 5. Full width at half maximum (FWHM) mass resolution characteristics of the EICS for four major magnetospheric ion constituents as a function of energy. The mass resolution at the 1% and 0.1% levels are typically degraded by factors of 1.8 to 2.2 and 2.4 to 2.8 respectively, dependent on both mass and energy.

maximum (FWHM) mass resolution as a function of energy for the four principal mass components of interest for the DE mission. The $^{16}O^+$ curves were derived by interpolating between $^{20}Ne^+$ and $^4He^+$. Due to the combined effects of preacceleration at low energies and defocusing at high energies, the response to differential number flux varies only slightly with mass and energy, ranging from 0.3 counts per s for a flux of one ion/(cm^2–sr–eV–s) at low energy, high mass to approximately 1.2 counts per s at high energy, low mass.

4. Data Formats and Analysis

The measurement of ion mass composition increases the complexity of data analysis and display formats. In general we must consider counting rate or differential flux as a function of time (or spacecraft position), pitch angle, energy and mass. Obviously all of these parameters cannot be presented in a single graph or with a single gray-scale. Therefore, in any presentation we must either sample in, or integrate over, one or more dimensions in parameter space. Except for detailed mass composition surveys it is reasonable to limit the dimensions of mass space to a few major constituents. Then each can be treated much like particle data without mass composition, such as those from electrostatic analyzers. For summary plots only $^1H^+$ and $^{16}O^+$ data are considered [12]. For each mass, fluxes are averaged over three representative energy ranges in each of 8 pitch angle ranges. The flux is plotted for the pitch angle at which it maximizes for each of the three energy ranges. For more detailed analysis, the simplest formats are line plots of individual components of flux versus one other parameter such as a differential flux spectrum. We also have the capability of generating several gray-scale plots. These include (1) flux versus energy and time for selected or averaged pitch angle ranges; (2) flux versus pitch angle and time for selected or averaged energy ranges; and (3) flux versus energy and pitch angle for selected or averaged time intervals. Lastly, we have the capability of plotting intensity versus mass step number for selected intervals. The latter will be used primarily for verification of the instrument mass response characteristics. In general no single format other than the summary plots will be run for all of the EICS data. The choice of detailed analysis format will be dependent on the particular problem under study. It will be posible for any investigator to call for any of the above formats to be run for a selected set of EICS data. Obviously the optimum format is dependent on the data acquisition mode.

Acknowledgments

The authors wish to express their appreciation for the cooperation and support of the DE project team during the development and integration of the EICS. In particular we wish to acknowledge the efforts of the instrument manager, Keith Fellerman, and the instrument engineer Marty Lidston, in solving the many parts and interface problems which otherwise would have made it extremely difficult to achieve success within the tight constraints of the DE project. We also wish to thank our co-investigators, R. G.

Johnson, R. D. Sharp, J. Geiss, P. Eberhardt, D. Young, and B. A. Whalen as well as the engineers, J. C. Bakke, V. F. Waltz, J. D. McDaniel, and S. Bjerklie for their efforts during the design, development and fabrication of the instrument. The Lockheed contributions to this effort were supported by NASA under contract NAS5-24302 and the University of Bern contributions were supported by the Swiss National Science Foundation under Grant 2.170.78.

References

1. Shelley, E. G., Johnson, R. G., and Sharp, R. D.: *Geophys. Res. Letter* **3**, 654 (1976).
2. Sharp, R. D., Johnson, R. G., and Shelley, E. G.: *J. Geophys. Res.* **82**, 3324 (1977).
3. Geiss, J., Balsiger, H., Eberhardt, P., Walker, H. P., Weber, L., Young, D. T., and Rosenbauer, H.: *Space Sci. Rev.* **22**, 537 (1978).
4. Peterson, W. K., Sharp, R. D., Shelley, E. G., Johnson, R. G., and Balsiger, H.: *J. Geophys. Res.* **86**, 761 (1981).
5. Sharp, R. D., Carr, D. L., Peterson, W. K., and Shelley, E. G.: *J. Geophys. Res.* **86**, 4639 (1981).
6. Kaye, S. M., Johnson, R. G., Sharp, R. D., and Shelley, E. G.: *J. Geophys. Res.* **86**, 1335 (1981).
7. Shelley, E. G., Sharp, R. D., and Johnson, R. G.: *J. Geophys. Res.* **81**, 2363 (1976).
8. Reiff, P. H., Hill, T. W., and Burch, K. L.: *J. Geophys. Res.* **82**, 479 (1977).
9. Shelley, E. G.: *Proceedings of the Sydney Chapman Conference, Alpbach*, ESA SP-148, **187** (1979).
10. Shelley, E. G., Sharp, R. D., Johnson, R. G., Geiss, J., Eberhardt, P., Balsiger, H., Haerendel, G., and Rosenbauer, H.: *IEEE Trans. on Geosci. Elect.* GE-16, 266 (1978).
11. Balsiger, H., Eberhardt, P., Geiss, J., Ghielmetti, A., Walker, H. P., Young, D. T., Loidl, H., and Rosenbauer, H.: *Space Sci. Instrument.* **2**, 499 (1976).
12. Smith, Paul H., Freeman, Clyde H., and Hoffman, R. A.: *Space Sci. Instrument.* **5**, 561 (1981) (this issue).